

# The Stability of Plasma-Sprayed $\text{MnCo}_2\text{O}_4$ Coatings at Elevated Temperature for Protective Application of Solid Oxide Fuel Cells

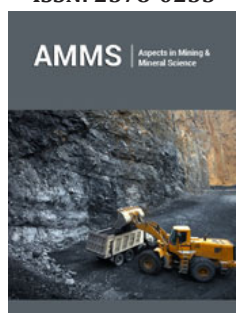
Zou J<sup>1,2</sup>, Wen K<sup>1</sup>, Song C<sup>1</sup>, Liu T<sup>1,\*</sup>, Deng C<sup>1</sup>, Liu M<sup>1</sup> and Yang C<sup>3</sup>

<sup>1</sup>Institute of New Materials, Guangdong Academy of Sciences, National Engineering Laboratory for Modern Materials Surface Engineering Technology, The Key Lab of Guangdong for Modern Surface Engineering Technology, China

<sup>2</sup>School of Materials Science and Engineering, Central South University, China

<sup>3</sup>School of Environment and Energy South China University of Technology, China

ISSN: 2578-0255



**\*Corresponding author:** Taikai Liu, Institute of New Materials, Guangdong Academy of Sciences, National Engineering Laboratory for Modern Materials Surface Engineering Technology, The Key Lab of Guangdong for Modern Surface Engineering Technology, China

**Submission:**  August 11, 2020

**Published:**  September 11, 2020

Volume 5 - Issue 4

**How to cite this article:** Zou J, Wen K, Song C, Liu T, Deng C, Liu M, Yang C. The Stability of Plasma-Sprayed  $\text{MnCo}_2\text{O}_4$  Coatings at Elevated Temperature for Protective Application of Solid Oxide Fuel Cells. *Aspects Min Miner Sci.* 5(4). AMMS. 000616. 2020.  
DOI: [10.31031/AMMS.2020.05.000616](https://doi.org/10.31031/AMMS.2020.05.000616)

**Copyright@** Taikai Liu, This article is distributed under the terms of the Creative Commons Attribution 4.0 International License, which permits unrestricted use and redistribution provided that the original author and source are credited.

## Abstract

As one of the most promising candidates to provide metallic interconnector the ability against oxidation at elevated temperature, conductible spinel has drawn a lot of attention in recent years. However, it is suffering poor stability during the preparation process, such as plasma spray. This work is proposed to concentrate on the preparation of highly conductible spinel coating.  $\text{MnCo}_2\text{O}_4$  spinel coatings are successfully obtained by atmospheric plasma spray. Conductivity test is carried out at 700°C with duration up to 15 hours. Stability and variation in microstructure are characterized by SEM, XRD, TEM and differential scanning calorimetry (DSC). Resultantly, coatings are found intensively densified that cracks and gaps are expelled, and number of pores is reduced. The as-sprayed coatings are found of more CoO and less  $\text{MnCo}_2\text{O}_4$ , while the densified coatings are composed of more  $\text{MnCo}_2\text{O}_4$  and less CoO. The measured conductivity of samples is 7.99S/cm, 4.00S/cm and 39.4S/cm for sample No.1, No.2 and No.3 respectively. Sample No.3 exhibit the best stability with the lowest specific heat flux of 0.8mW/mg and the biggest average grain size of 227nm while the specific heat flux of sample No.2 is as high as 1.8mW/mg and the average grain size is 83nm. Both the densification, phase composition and the grain size contribute to the conductivity of the coatings.

**Keywords:**  $\text{MnCo}_2\text{O}_4$  spinel; Metallic interconnect; SOFC; Conductivity; Densification; Phase composition

## Introduction

As one of the most important components of SOFC stack, interconnector provides current conduction, thermal conduction and mechanic support to cells. Replacing ceramic interconnector, such as  $\text{LaCrO}_3$ , by metallic interconnector allows lower operating temperature of SOFC. Due to the relatively low cost, good workability and excellent resistance to thermal oxidation, ferritic stainless steel is considered as the most promising candidates of interconnector materials. However, the use of ferritic stainless steel also brings problems, the existence of Chromium oxide ( $\text{Cr}_2\text{O}_3$ ) causing higher ohmic resistance [1] and the evaporation of Chromium to cathode leading to cell performance degradation [2-4]. Spinel has been intensively studied as promising protective coating [5-11]. However, currently most of the methods to prepare Mn-Co spinel coating either costs too high, or deposits too slow, or is of low scalability. Plasma spray, as a surface modification technology, has been widely used to fabricate coatings on surface to endure production new properties [12,13]. However, for maintaining the performance of SOFC stack, the protective spinel coating shall be thin, dense and stable. Hu et al. [14] successfully applied plasma spray to prepare Mn-Co spinel coating [14]. The measured ASR of coated metallic interconnector is as low as 13mWcm<sup>2</sup> after sintered at 800 °C for 200h, whilst the spinel coating is 100µm thick. Moreover, the spinal phase is suffering the poor stability when exposed to hot plasma. Therefore, this work is proposed to study the influence of thermal condition during the preparation on spinal coatings and clarify the effect of heating treatment on the microstructure of spinal coatings. In this work, commercial spinal powder is used as raw material to prepare spinal coatings by plasma spray process.  $\text{MnCo}_2\text{O}_4$  spinel coatings are obtained with controlled spray conditions. The conductivity of obtained  $\text{MnCo}_2\text{O}_4$  spinel coatings are measured. The stability and microstructure of spinal coatings are characterized. The effect of heating treatment on spinal coatings is estimated.

## Methodology and Methods

### Coating preparation

Three sets of spinal coatings are obtained by atmospheric plasma spray. The setup of the spray system is described elsewhere [15]. The raw material used is spherical  $Mn_{1.5}Co_{1.5}O_4$  powder with average diameter of  $28.5\mu m$ . The spinal powder is fed at a rate of 20g/min. Ceramic sheets with dimension of  $1.85cm \times 2mm$  are employed as substrate to allow conductivity measurement. More details are available in (Table 1).

**Table 1:** Parameters to prepare coatings and the thickness of obtained coatings.

	Gas (L/min)	Current (A)	Power (kW)	Thickness ( $\mu m$ )
No. 1	65	500	40	$19 \pm 5$
No. 2	50	700	48	$20 \pm 5$
No. 3	90	700	62	$21 \pm 5$

### Conductivity measurement

The four-point method is employed to measure the conductivity of obtained coatings. The testing sample is placed in a tubular furnace with  $\phi 50mm$  orifice at two ends. All measurements are performed at  $700^\circ C$  with duration up to 15 hours. Constant current of 0.2A is applied, the corresponding voltage is recorded for conductivity calculation according to a method reported in the literature [16].

### Characterizations

30mg of raw powder and obtained samples are placed in  $Al_2O_3$  crucible for DSC test. The test was performed from room temperature to  $800^\circ C$  with heating rate of  $5^\circ C/min$ . The test chamber was protected by Argon (99.99%). Phase composition and micromorphology of raw powder and coatings are characterized by XRD, SEM and TEM.

## Results and Discussion

Confirmed by XRD, the raw powder consisted of  $MnCo_2O_4$  (PDF#23-1237) and  $Mn_{1.5}Co_{1.5}O_4$  (PDF#18-0409) as shown in Figure 1. The phase of  $Mn_{1.5}Co_{1.5}O_4$  is considered as a mixture of  $Mn_3O_4$  and  $Co_3O_4$ , both of which belong to F3dm space group. Since both  $Co_3O_4$  and  $Mn_3O_4$  are unstable at elevated temperature, the as-sprayed samples are found with CoO (PDF#74-2392) and  $MnCo_2O_4$  [17]. The existence of thermal stress results a shift of the diffraction peaks toward the lower  $2\theta$  angles. The shift of sample No.1-as and No.2-as is about 1 degree, while for sample No.3-as the shift angle is about 0.8 degree. After tested at  $700^\circ C$  for 15 hours, spinal phase and  $Al_2O_3$  (PDF#42-1468) from the substrate are detected in the coatings for all samples (Figure 1). A weak peak of CoO is also found after the conductivity test, especially the peak at  $61.8^\circ$ . By absorbing oxygen, the majority of CoO turned to spinel phase after the conductivity test. The diffraction peaks of  $MnCo_2O_4$  are wider and weaker in sample No.2 than that of others ("tt" means "tested"). It means a poor crystallization of  $MnCo_2O_4$  phase, and thus less  $MnCo_2O_4$  phase is presented. The morphology of as-sprayed samples and tested samples are presented in (Figure 2) as well as the TEM diffraction pattern and HRTEM of sample No. 3. The as-sprayed coatings are found composed of cracks, gaps and pores, which are due to the poor melt of raw particles. Due to the relatively low temperature or the shortness of the plasma plume, it's insufficient to completely melt all raw particles and hence partially melted particles and fully melted particles coexist in the obtained coatings. However, by controlling the input plasma power, no obvious difference was observed between coatings. No visible change of microstructure presents by increasing the flowrate of plasma gas. However, by conducting the conductivity test at  $700^\circ C$ , coatings are significantly densified as shown in Figure 2. Checked by TEM diffraction, the densified coatings were  $MnCo_2O_4$  (spinel) with an interplanar spacing of 0.288nm.

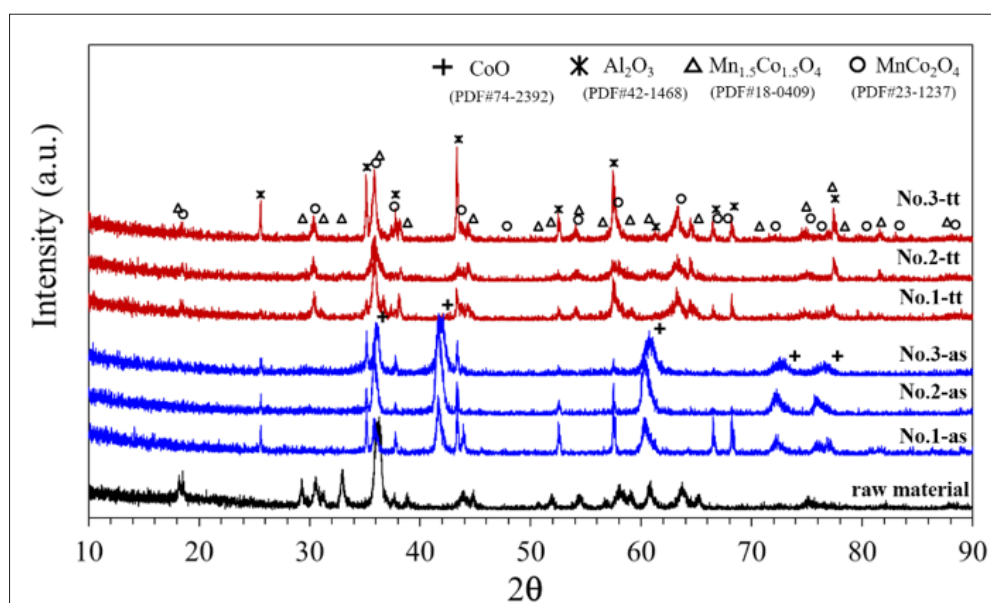


**Figure 1:** XRD spectrum of raw powder, as-sprayed samples and tested samples.

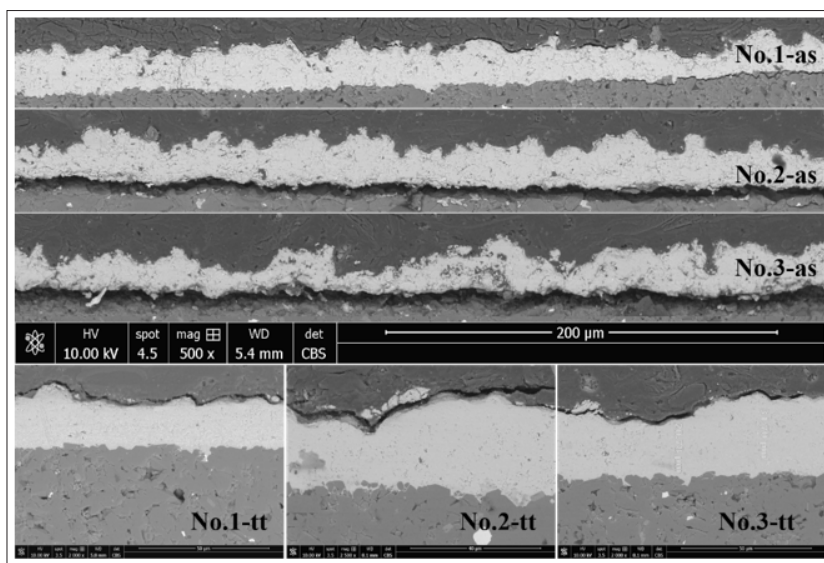


**Figure 2:** Micromorphology and TEM diffraction pattern of samples.

As shown in Figure 3(a), from room temperature to 800 °C, the thermal behavior of as-sprayed coatings is characterized. Exothermic peak is observed for all samples between 630 °C-720 °C that means the selection of testing temperature of conductivity is reasonable. Moreover, the maximal specific thermal flux of sample No.1 is 0.95mW/mg and for No. 2 it is 1.8mW/mg, while for sample No. 3 it is only 0.8mW/mg. Obviously, sample No. 5 presents the most excellent stability and sample No. 2 is of the poorest stability. As presented in Figure 3(b), sample No.1 and No.3 are found with a low mass augmentation about 3% at 800 °C while sample No.2 exhibits a higher mass augmentation of 5%. It means more oxygen is absorbed by sample No.2 to compensate the oxygen loss during the preparation. It also means the coating of sample No.2 experiences serious deoxidization. According to the phase diagram of  $Mn_3O_4$ - $Co_3O_4$ ,  $(Mn,Co)O$  is the main product of deoxidization of  $(Mn, Co)_3O_4$  spinel. Listed in (Table 2) is the conductivity ( $\rho$ ) of coatings and the coefficient (c) to calculate the conductivity obtained according to method reported in literature [16]. The conductivity is obtained

as  $\rho=cI/U$ . Sample No. 3 shows the highest conductivity of 39.40S/cm, sample No. 2 exhibits the lowest conductivity of 4.00S/cm and the conductivity of sample No.1 is 7.99S/cm. As the measurement is conducted at 700 °C for 15 hours, densification happens that the densified coatings are found free of cracks, gaps and with reduced number of pores, thus the resistance from defects is highly diminished. It is well known that the conductivity of conductive spinel is in form of electron hopping. With less cracks/gaps/interlayers, the interfacial barrier is thus dramatically lowered that more electrons can hop between adjacent sites to provide a high conductivity.

**Table 2:** Conductivity of coatings obtained at 700 °C in air.

	I (A)	U (V)	C (cm <sup>-1</sup> )	$\rho$ (S/cm)
No.1	0.2	1.38	55.16	7.99
No.2	0.2	2.76	55.16	4.00
No.3	0.2	0.28	55.16	39.40

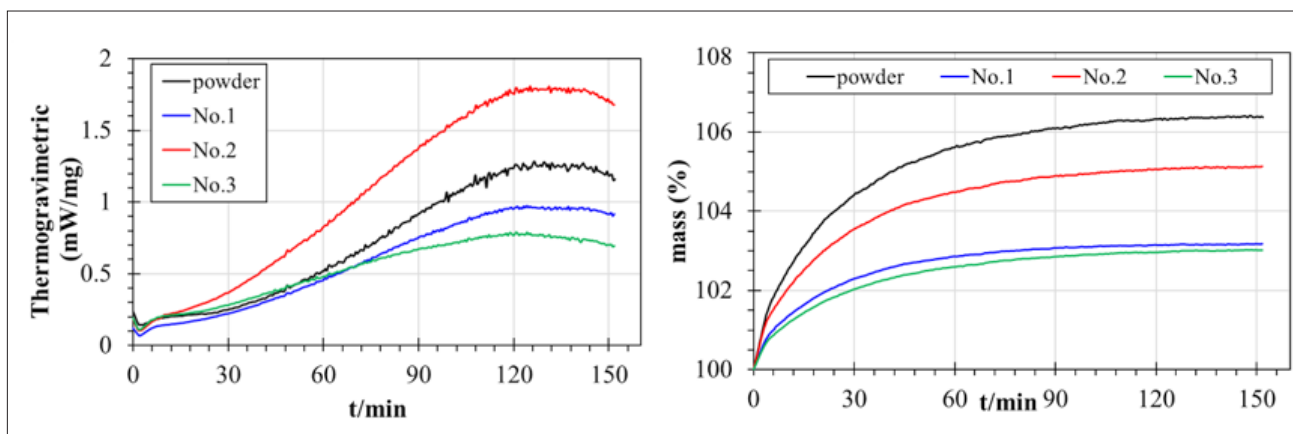


**Figure 3:** (a) The plots of specific thermal flux and (b) mass augmentation of tested coatings.

After conductivity measurement, the microstructure of tested samples is checked by TEM-SEM (Figure 4). Average grain size is calculated from XRD diffraction data according to Scherrer's method. The grains size of tested samples is 120nm, 83nm and 227nm for sample No.1, No.2 and No.3 respectively. As shown in Figure 4, the grain of sample No.2-tt is obviously smaller than that of sample No.3-tt. More important, the grain boundaries in of sample No.3-tt are faded out that grains grow together forming sub-grains. The difference in grain size is coincided with the change

of conductivity. It is well accepted that the bigger the grain is, the less the boundary presents. With the biggest grain size, sample No. 3 exhibited the least grain boundary and thus the lowest interfacial resistance for hopping conduction. Sample No. 2 shows the smallest grain size, and thus the most interfacial barrier. Moreover, the phase composition also contributed to the conductivity. Sample No.2 is found with the least  $\text{MnCo}_2\text{O}_4$  phase while the diffraction peaks of  $\text{MnCo}_2\text{O}_4$  of sample No.3 is sharp and intensive the conductivity. It is coincided with the measured conductivity as shown in Table 2.

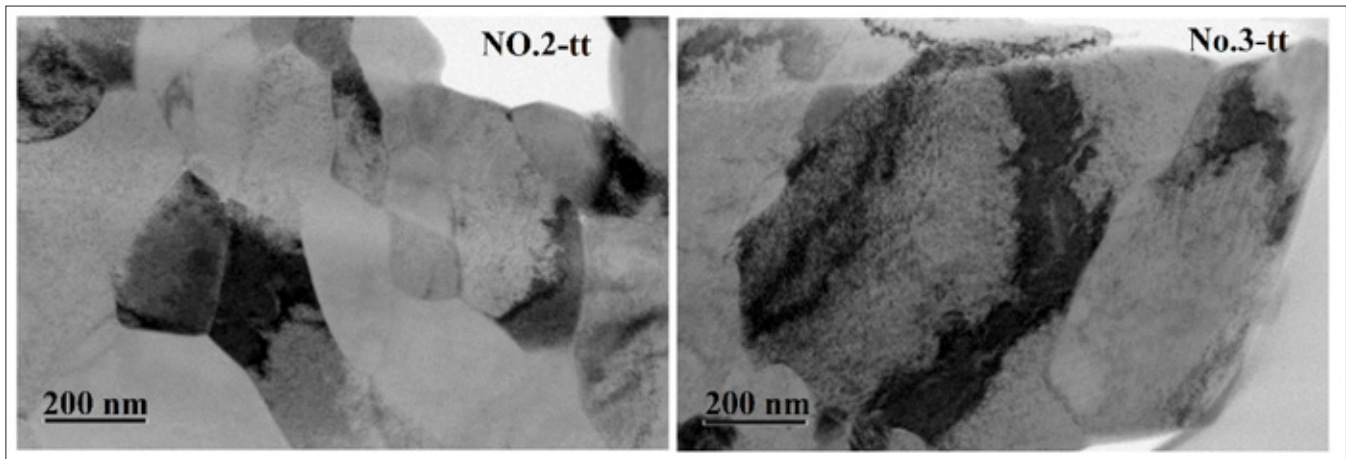


**Figure 4:** Microstructure of sliced samples prepared by FIB of tested sample No.2 and No.3.

## Conclusion

In conclusion,  $\text{MnCo}_2\text{O}_4$  coatings are successfully prepared by atmospheric plasma spray with controlled condition. The as-sprayed coatings consist of cracks, gaps and pores. The composition of the as-sprayed coatings is identified as CoO and a little  $\text{MnCo}_2\text{O}_4$ . The presence of CoO is considered as the result of deoxidization of spinel phase in the raw material. By applying thermal stage at 700 °C for 15 hours, a densification effect is found over these coatings, that cracks, gaps and pores are strongly diminished leaving a dense coating. The densified coating is found composed of  $\text{MnCo}_2\text{O}_4$  and a small amount of CoO. Sample No. 3 exhibits the best stability with specific thermal flux of 0.8mW/mg and thus the best conductivity of 39.40S/cm while sample No. 2 exhibits the highest specific thermal flux of 1.8mW/mg and thus the lowest conductivity of 4S/cm. Densification, grain size and phase composition are considered contributed to the conductivity.

## Acknowledgement

This work is supported by the following projects: National Key R&D Program of China (2018YFB1502600), Platform construction project of modern material surface engineering technology innovation for industrial applications (2018GDASCX-0111), technology cultivation and innovation project of modern material surface engineering (2019GDASYL-0402004), Guangdong Science and Technology Plan Project (2017A070701027) and Guangdong Special Support Program (2019BT02C629).

## References

- Brandner M, Bram M, Froitzheim J, Buchkremer HP, Stöver D (2008) Electrically conductive diffusion barrier layers for metal-supported SOFC. *Solid State Ion* 179: 1501-1504.
- Yang Z, Guo M, Wang N, Ma C, Wang J, et al. (2017) A short review of cathode poisoning and corrosion in solid oxide fuel cell. *International Journal of Hydrogen Energy* 42(39): 24948-24959.
- Menzler NH, Sebold D, Wessel E (2014) Interaction of  $\text{La}_{0.58}\text{Sr}_{0.40}\text{Co}_{0.20}\text{Fe}_{0.80}\text{O}_{3-\delta}$  cathode with volatile Cr in a stack test-scanning electron microscopy and transmission electron microscopy investigations. *Journal of Power Sources* 254: 148-152.
- Yang M, Bucher E, Sitte W (2011) Effects of chromium poisoning on the long-term oxygen exchange kinetics of the solid oxide fuel cell cathode materials  $\text{La}_{0.6}\text{Sr}_{0.4}\text{CoO}_3$  and  $\text{Nd}_2\text{NiO}_4$ . *Journal of Power Sources* 196: 7313-7317.
- Liu H, Zhu X, Cheng M, Cong Y, Yang W (2011) Novel  $\text{Mn}_{1.5}\text{Co}_{1.5}\text{O}_4$  spinel cathodes for intermediate temperature solid oxide fuel cells. *Chemical Communication Cambridge England* 47(8): 2378-2380.
- Yang Z, Xia G, Stevenson JW (2005)  $\text{Mn}_{1.5}\text{Co}_{1.5}\text{O}_4$  spinel protection layers on ferritic stainless steels for SOFC interconnect applications. *Electrochemical Solid-State Letter* 8(3): A168-A170.
- Acharyya SS, Ghosh S, Adak S, Sasaki T, Bal R (2014) Facile synthesis of  $\text{CuCr}_2\text{O}_4$  spinel nanoparticles: A recyclable heterogeneous catalyst for the one pot hydroxylation of benzene. *Catalysis Science Technology* 4: 4232-4241.
- Molin S, Jasinski P, Mikkelsen L, Zhang W, Chen M, et al. (2016) Low temperature processed  $\text{MnCo}_2\text{O}_4$  and  $\text{MnCo}_{1.8}\text{Fe}_{0.2}\text{O}_4$  as effective protective coatings for solid oxide fuel cell interconnects at 750 °C. *Journal of Power Sources* 336: 408-418.

9. Kruk A, Stygar M, Brylewski T (2013) Mn-Co spinel protective-conductive coating on AL<sub>453</sub> ferritic stainless steel for IT-SOFC interconnect applications. *Journal of Solid State Electrochemistry* 17: 993-1003.
10. Hashemi ST, Dayaghi AM, Askari M, Gannon PE (2018) Sol-gel synthesis of Mn<sub>1.5</sub>Co<sub>1.5</sub>O<sub>4</sub> spinel nano powder for coating applications. *Materials Research Bulletin* 102: 180-185.
11. Mardare CC, Spiegel M, Savan A, Ludwig A (2009) Thermally oxidized Mn-Co thin films as protective coatings for SOFC interconnects. *Journal of Electrochemistry Society* 156: B1431-B1439.
12. Hui R, Wang Z, Kesler O, Rose L, Jankovic J, et al. (2007) Thermal plasma spraying for SOFCs: Applications, potential advantages, and challenges. *J Power Sources* 170(2): 308-323.
13. McPherson R (1989) A review of microstructure and properties of plasma sprayed ceramic coatings. *Surf Coat Technol* 39-40: 173-181.
14. Hu YZ, Yao SW, Li CX, Li CJ, Zhang SL (2017) Influence of pre-reduction on microstructure homogeneity and electrical properties of Mn<sub>1.5</sub>Co<sub>1.5</sub>O<sub>4</sub> coatings for SOFC interconnects. *International Journal of Hydrogen Energy* 42(44): 27241-27253.
15. Liu T, Arnold J (2016) Study of in-flight particle stream and particle behavior for understanding the instability phenomenon in plasma spraying process. *Surf Coat Technol* 286: 80-94.
16. Miccoli I, Edler F, Pfnür H, Tegenkamp C (2015) The 100<sup>th</sup> anniversary of the four-point probe technique: The role of probe geometries in isotropic and anisotropic systems. *J Phys Condens Matter* 27(22): 223201.
17. Aukrust E, Muan A (2006) Phase relations in the system cobalt oxide-manganese oxide in air. *J Am Ceram Soc* 46(10): 511.

For possible submissions Click below:

Submit Article